Commun Nonlinear Sci Numer Simulat 35 (2016) 137–147

Contents lists available at ScienceDirect

Commun Nonlinear Sci Numer Simulat

journal homepage: www.elsevier.com/locate/cnsns

Transmission dynamics of schistosomiasis in Zimbabwe: A mathematical and GIS Approach

E.T. Ngarakana-Gwasira [a], C.P. Bhunu [a,*], M. Masocha [b], E. Mashonjowa [c]

[a] Department of Mathematics, University of Zimbabwe, P. O. Box MP167 Mount Pleasant, Harare, Zimbabwe
[b] Department of Geography, University of Zimbabwe, P. O. Box MP167 Mount Pleasant, Harare, Zimbabwe
[c] Department of Physics, University of Zimbabwe, P. O. Box MP167 Mount Pleasant, Harare, Zimbabwe

ARTICLE INFO

Article history:
Received 12 March 2014
Revised 24 June 2015
Accepted 9 November 2015
Available online 15 November 2015

Keywords:
Schistosomiasis
GIS
Reproduction number

ABSTRACT

Temperature and presence of water bodies are known to influence the transmission dynamics of schistosomiasis. In this work, effects of water bodies (taken in context of rainfall patterns) and temperature from 1950 to 2000 are considered in the model. With the aid of Geographic Information System (GIS), the reproduction number is mapped on the Zimbabwean country. Results of the mapping show high reproduction numbers along the Lowveld and the Zambezi valley catchment area. High reproduction numbers suggest high levels of schistosomiasis. This result suggests more control efforts should be targeted in these areas with high reproduction numbers.

1. Introduction

Schistosomiasis also referred to as bilharzias (or snail fever) is an infectious disease caused by parasitic flatworms of the genus schistosoma. It is a major source of morbidity affecting over 250 million people worldwide, with 85% occurring in the developing tropical countries in Africa, Asia, South America and the Middle East [1,2]. In terms of morbidity and mortality, schistosomiasis is considered the second most important human parasitic disease after malaria [3]. Schistosomiasis continues to drain the socio-economic development of already impoverished rural communities of sub-Saharan Africa.

Schistosomiasis may localise in different parts of the body and its localisation determines its particular clinical profile [4]. Schistosomiasis is caused by five species of flatworms, each of which causes a different clinical presentation of the disease. Intestinal schistosomiasis is caused by Schistosoma mansoni, urinary schistosomiasis is caused by Schistosoma haematobium and Schistosoma japonicum and Schistosoma mekongi cause Asian intestinal schistosomiasis [5]. Three species of schistosomiasis, S. haematobium (prevalent in Africa), S. japonicum (prevalent in Japan, Southeast Asia, and Western Pacific) and S. mansoni (prevalent in Africa, Southwest Asia, Brazil and the Caribbean) are responsible for the majority of schistosomiasis infection while the other two species, S. intercalatum and S. mekongi parasitise humans to a much lesser extent [6]. Flatworms infect humans by penetrating the skin when exposed to contaminated freshwater (e.g., when wading, swimming, or bathing). The flatworms spread in freshwater areas, such as rivers and lakes, where freshwater snails act as intermediate hosts for the parasite's larvae. As such, the habitats of the host snails are of great importance for the spread of the disease. The most important determinants of the population dynamics of snails are temperature and rainfall [4]. The best survival temperature of snails was found to be between 20 °C and 25 °C while at 40 °C none of the snails survived [8]. However, snails are less sensitive to low temperatures

* Corresponding author. Tel.: +263 736018918.
E-mail address: cpbhunu@gmail.com, cp-b@hotmail.co.uk (C.P. Bhunu).

http://dx.doi.org/10.1016/j.cnsns.2015.11.005
1007-5704/

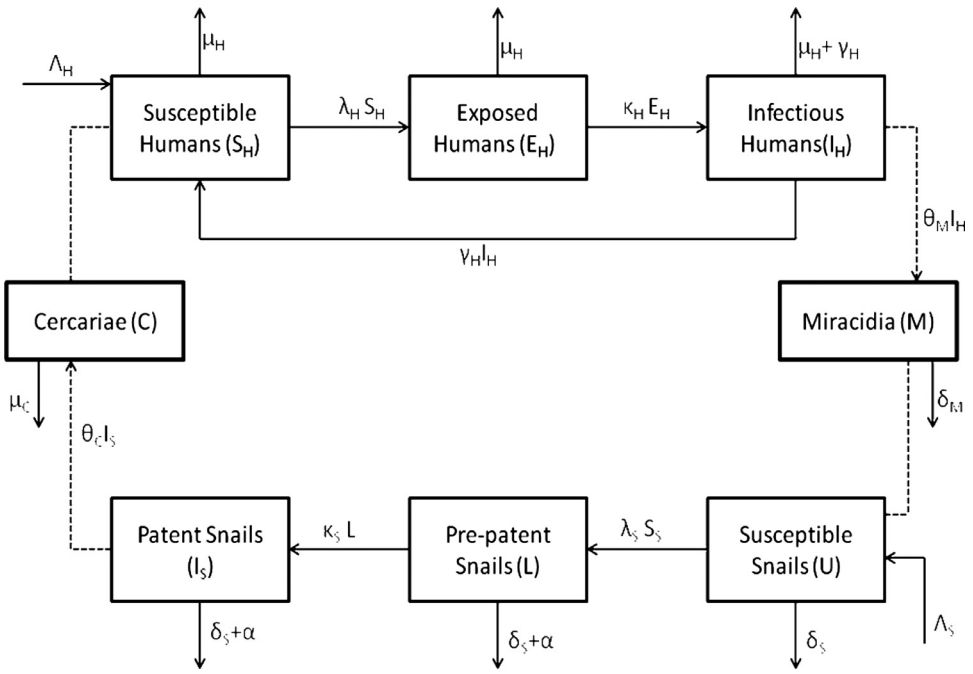

Fig. 1. Model diagram of the mathematical model for schistosomiasis transmission. Dotted lines on the diagram denote indirect interaction.

than schistosome parasites in snails. Uninfected snails can therefore be found in high altitude areas of endemic countries where low temperatures inhibit larval development in snails [7]. Dagal et al. [8] considered the effects of water temperatures on hatchability of eggs and survival of snails and found that at low temperatures 15 °C, none of the eggs hatched. The mean survival rate of snails between 5 °C and 10 °C was found to be zero. As temperature increased, hatching rate increased but at 35 °C none of the eggs hatched.

Incorporating climate effects into models of disease dynamics is now extremely important as there is a strong need to understand the effects of climate change. The schistosome and snail life cycles are highly dependant on ambient conditions and climate change is known to affect several parameters in the epidemiology of schistosomiasis. Developing an epidemiological model to predict how these factors bring out the impact of climate on the dynamics of schistosomiasis transmission is crucial. Here, a schistosomiasis model is incorporated into geographic information systems (GIS) to get a feel of the possible variation of schistosomiasis intensity in Zimbabwe.

2. Model formulation

The life cycle of schistosome parasites is complicated and involves two different hosts: human beings and snails. A model to trace the life cycle of schistosome parasite is formulated. The model is based on monitoring the dynamics of the populations at any time t of susceptible humans $S_H(t)$, exposed humans $E_H(t)$, infectious humans I_H, miracidia $M(t)$ (larvae of the parasite soon after hatching from the eggs), uninfected snails $U(t)$, latently infected snails $L(t)$, patent infected snails (infected snails not yet releasing cercariae) $I_s(t)$ and cercariae $C(t)$ (larvae released into the water from infected snail ready to enter the human skin). Individuals are recruited into the human population at a rate Λ_H. Susceptible individuals acquire infection at a rate $\lambda_H = \frac{\beta_H C(t)}{C_0+\epsilon C(t)}$, where β_H is the cercarial infection rate, C_0 is a saturation constant for the cercariae and ϵ is the limitation of the growth velocity of cercariae with the increase of cases. Upon infection, an individual does not automatically become infectious but enters an exposed class as the incubation period of schistosomiasis ranges from 4 to 8 weeks for schistosomiasis mansoni and schistosomiasis japonicum, respectively [9,10]. Individuals then progress to the infectious compartment at a rate κ_H. Susceptible and infected individuals suffer from natural death rate μ_H, but infectious individuals have an additional host mortality δ_H. Adult schistosomes within infected human hosts produce eggs which hatch and develop to free-swimming miracidia at a net rate θ_M. Miracidia either die at a rate δ_M or infect uninfected snails at rate $\lambda_S = \frac{\beta_S M}{M_0+\epsilon M}$. Adult snails are recruited into the susceptible snail population at a rate Λ_S. Upon infection, snails enter the latently infected class from which they progress to the patent infected class at a rate κ_S. Adult snails die naturally at rate δ_S and infected adult snails also die due to parasite-induced mortality at an additional rate α. The patent infected snails will then release a second form of free swimming larvae called cercariae at a rate θ_C which is capable of infecting humans. Cercariae die naturally at the rate δ_C.

A compartmental model of schistosomiasis dynamics is presented in Fig. 1.

The following system of differential equations describes the model:

$$\begin{aligned}
S_H'(t) &= \Lambda_H - \frac{\beta_H C S_H}{C_0 + \epsilon C} - \mu_H S_H + \gamma_H I_H,\\
E_H'(t) &= \frac{\beta_H C S_H}{C_0 + \epsilon C} - (\kappa_H + \mu_H) E_H,\\
I_H'(t) &= \kappa_H E_H - (\mu_H + \delta_H + \gamma_H) I_H,\\
M'(t) &= \theta_M I_H - \frac{\beta_S M U}{M_0 + \epsilon M} - \delta_M M,\\
U'(t) &= \Lambda_S - \frac{\beta_S M U}{M_0 + \epsilon M} - \delta_S U,\\
L'(t) &= \frac{\beta_S M U}{M_0 + \epsilon M} - (\delta_S + \alpha + \kappa) L,\\
I_S'(t) &= \kappa L - (\delta_S + \alpha) I_S,\\
C'(t) &= \theta_C I_S - \frac{\beta_H C S_H}{C_0 + \epsilon C} - \delta_C C.
\end{aligned} \tag{1}$$

where $A_1 = 351.04480681884,\ A_2 = -1925.49534415329,\ A_3 = -85.1815135926783,\ B_1 = -8.59,$
$B_2 = 855,\ B_3 = 31487.35,\ B_4 = 574921.12, B_5 = 5188906,\ B_6 = 18196700,\ C_1 = 11.4267,$
$C_2 = 126.89,\ C_3 = 525.29, C_4 = -960.38,\ C_5 = 654.3,\ D_1 = -1.333627E-02,\ G_1 = 6.45,$
$D_2 = 8.738295237E-06,\ D_3 = 1334.208298\ F_1 = 3.99E-07,\ F_2 = -3.73E-05,\ F_3 = 4.97E-04,$
$F_4 = 3.99E-02,\ F_5 = -1.149,\ F_6 = 9.59,\ G_2 = 40.19,\ G_3 = -907.85,\ H_1 = 2.97E-06,$
$H_2 = -3.699E-04,\ H_3 = 1.83E-02,\ H_4 = -0.45,\ H_5 = 5.38,\ H_6 = -25.688$
$a = 0.23,\ b = -1.05,\ B_m = 0.849,\ T_m = 25$

We make a simplification common in models with free living particles and assume that the rate of the particle depletion by hosts or snails has negligible impact on particle dynamics [11]. This is done to reduce the complexity of the mathematics involved. In this case the interaction between the miracidia and the susceptible snail $\frac{\beta_S M U}{M_0+\epsilon M}$ and the interaction between the cercariae and the humans $\frac{\beta_H C S_H}{C_0+\epsilon C}$ are assumed to be negligible on pathogen dynamics. System (1) can now be written as

$$\begin{aligned}
S_H'(t) &= \Lambda_H - \frac{\beta_H C S_H}{C_0 + \epsilon C} - \mu_H S_H + \gamma_H I_H,\\
E_H'(t) &= \frac{\beta_H C S_H}{C_0 + \epsilon C} - (\kappa_H + \mu_H) E_H,\\
I_H'(t) &= \kappa_H E_H - (\mu_H + \delta_H + \gamma_H) I_H,\\
M'(t) &= \theta_M I_H - \delta_M M,\\
U'(t) &= \Lambda_S - \frac{\beta_S M U}{M_0 + \epsilon M} - \delta_S U,\\
L'(t) &= \frac{\beta_S M U}{M_0 + \epsilon M} - (\delta_S + \alpha + \kappa) L,\\
I_S'(t) &= \kappa L - (\delta_S + \alpha) I_S,\\
C'(t) &= \theta_C I_S - \delta_C C.
\end{aligned} \tag{2}$$

All feasible solutions of model system (2) enter the region

$$\Omega = \begin{cases}
(S_H, E_H, I_H) \in \mathbb{R}_+^3 : N_H \le \dfrac{\Lambda_H}{\mu_H},\\
M \in \mathbb{R}_+ : M \le \dfrac{\theta_M \Lambda_H}{\delta_M \mu_H},\\
(U, L, I_S) \in \mathbb{R}_+^3 : N_S \le \dfrac{\Lambda_S}{\delta_S},\\
C \in \mathbb{R}_+ : C \le \dfrac{\theta_C \Lambda_S}{\delta_C \delta_S},
\end{cases} \tag{3}$$

which is positively invariant and attracting and it is sufficient to consider solutions in Ω. Existence, uniqueness and continuation results for system (2) hold in this region and all solutions starting in Ω remain in there for all $t \ge 0$. Hence, (2) is mathematically and epidemiologically well-posed and it is sufficient to consider the dynamics of the flow generated by the model system (2) in Ω. Also, all parameters and state variables for model system (2) are assumed to be non-negative since it monitors human, snail, miracidia and cercariae populations.

Table 1
Parameters of the basic schistosomiasis transmission model in Eq. (1) where T represents temperature and P represents rainfall. [a]* denotes temperature dependant parameters designed using Datafit based on results from [a].

Description	Symbol	Value	Source
Recruitment rate of humans	Λ_H	8000	[11]
Cercarial infection rate	β_H	$-2.296 + 0.446 \ln T + \frac{2.96}{\ln T}$	[14]*
Saturation constant of cercariae	C_0	9000000	[11]
Progression rate of humans	κ_H	0.017857	est
Natural death rate of humans	μ_H	0.014	[12]
Disease induced human death rate	δ_H	0.039	[11]
Adult snail recruitment rate	$\Lambda_S(T)$	$100e^{A_1 + \frac{A_2}{T} + A_3 \ln T}$	[14]*
Adult snail recruitment rate	$\Lambda_S(T,P)$	$80B_m \frac{e^{-c[T-T_m]^2}}{1+e^{a-bP}}$	[13]*
Miracidia infection rate	β_S	$B_1 + \frac{B_2}{T} - \frac{B_3}{T^2} + \frac{B_4}{T^3} - \frac{B_5}{T^4} + \frac{B_6}{T^5}$	[8]*
Saturation constant for the miracidia	M_0	100000000	[11]
Adult snail mortality rate	δ_S	$C_1 - \frac{C_2}{\ln T} + \frac{C_3}{(\ln T)^2} + \frac{C_4}{(\ln T)^3} + \frac{C_5}{(\ln T)^4}$	[14]*
Additional snail mortality due to infection	α	$D_1 + D_2 T^{2.5} + D_3 e^{-T}$	[14]*
Net miracidial production rate	θ_M	500	[14]*
Miracidial death rate	δ_M	$F_1 T^5 + F_2 T^4 + F_3 T^3 + F_4 T_5^F T + F_6$	[14]*
Cercarial production rate	θ_C	$G_1 T^2 + G_2 T + G_3$	[14]*
Cercarial mortality rate	δ_c	0.004	[13]
Within snail schistosome maturation rate	κ_S	$H_1 T^5 + H_2 T^4 + H_3 T^3 + H_4 T^2 + H_5 T + H_6$	[14]*

3. Equilibrium states

The equilibrium states of the basic model are obtained by setting the right hand side of system (2) to zero. Model system (2) has two steady states.

3.1. The disease free equilibrium

The parasite larval stages (represented by M and C) have relatively short lifespans compared with those of worms, humans and snails. So the dynamic equations for M and C are replaced with their quasi-equilibrated values $C^* = \frac{\theta_C I_S}{\delta_S}$ and $M^* = \frac{\theta_M I_H}{\delta_M}$. The original system (2) is reduced to a six dimensional form for variables S_H, E_H, I_H, U, L and I_S.

$$\begin{aligned}
S_H'(t) &= \Lambda_H - \frac{\beta_H S_H \frac{\theta_C I_S}{\delta_S}}{C_0 + \epsilon \frac{\theta_C I_S}{\delta_S}} - \mu_H S_H + \gamma_H I_H,\\
E_H'(t) &= \frac{\beta_H S_H \frac{\theta_C I_S}{\delta_S}}{C_0 + \epsilon \frac{\theta_C I_S}{\delta_S}} - (\mu_H + \kappa_H) E_H,\\
I_H'(t) &= \kappa_H E_H - (\mu_H + \delta_H + \gamma_H) I_H,\\
U'(t) &= \Lambda_S - \frac{\beta_S U \frac{\theta_M I_H}{\delta_M}}{M_0 + \epsilon \frac{\theta_M I_H}{\delta_M}} - \delta_S U,\\
L'(t) &= \frac{\beta_S U \frac{\theta_M I_H}{\delta_M}}{M_0 + \epsilon \frac{\theta_M I_H}{\delta_M}} - (\delta_S + \alpha + \kappa) L,\\
I_S'(t) &= \kappa L - (\delta_S + \alpha) I_S.
\end{aligned} \tag{4}$$

At the disease free equilibrium, there are no infected humans and infected snail, thus the model system (4) has a disease free equilibrium

$$\mathcal{E}_0 = (S_H, E_H, I_H, U, L, I_S) = \left(\frac{\Lambda_H}{\mu_H}, 0, 0, \frac{\Lambda_S}{\delta_S}, 0, 0 \right)$$

3.2. Basic reproduction number

The next generation operator approach as described by Diekmann et al. [15] is used to define the treatment induced reproductive number, $\mathcal{R}_s$, as the number of new infections (in snails or humans) produced by one infectious individual or snail over the duration of the infectious period in the presence of treatment for infected humans.

$$\mathcal{R}_s = \sqrt{\frac{\kappa_H \kappa_S \beta_H \theta_C \Lambda_H \beta_S \theta_M \Lambda_S}{\delta_c C_0 \delta_H \delta_M M_0 \delta_S (\kappa_H + \mu_H)(\delta_S + \alpha + \kappa_S)(\delta_S + \alpha)(\mu_H + \delta_H + \gamma_H)}}. \tag{5}$$

3.3. Local stability of the disease-free equilibrium $\mathcal{E}_0$

The local stability of the disease free equilibrium can be discussed by examining the linearised form of the system (4) at the steady state $\mathcal{E}_0$.

Theorem 1. *The disease-free equilibrium $\mathcal{E}_0$ is locally asymptotically stable whenever $\mathcal{R}_s < 1$, and unstable otherwise.*

Proof. The Jacobian matrix of the model (4) evaluated at the disease free equilibrium point is given by

$$\begin{bmatrix} -\mu_H & 0 & \gamma_H & 0 & 0 & -\frac{\beta_H\theta_C\Lambda_H}{\delta_C C_0\delta_H} \\ 0 & -(\kappa_H+\mu_H) & 0 & 0 & 0 & \frac{\beta_H\theta_C\Lambda_H}{\delta_C C_0\delta_H} \\ 0 & \kappa_H & -(\mu_H+\delta_H+\gamma_H) & 0 & 0 & 0 \\ 0 & 0 & -\frac{\beta_S\theta_M\Lambda_S}{\delta_M M_0\delta_C} & -\delta_S & 0 & 0 \\ 0 & 0 & \frac{\beta_S\theta_M\Lambda_S}{\delta_M M_0\delta_C} & 0 & -(\delta_S+\alpha+\kappa_S) & 0 \\ 0 & 0 & 0 & 0 & \kappa_S & -(\delta_S+\alpha) \end{bmatrix}.$$

The first and the fourth columns have diagonal entries resulting in these diagonal entries being two of the eigenvalues of the Jacobian matrix. Now excluding these columns and the corresponding rows we calculate the remaining eigenvalues.

$$\begin{bmatrix} -(\kappa_H+\mu_H) & 0 & 0 & \frac{\beta_H\theta_C\Lambda_H}{\delta_C C_0\delta_H} \\ \kappa_H & -(\mu_H+\delta_H+\gamma_H) & 0 & 0 \\ 0 & \frac{\beta_S\theta_M\Lambda_S}{\delta_M M_0\delta_C} & -(\delta_S+\alpha+\kappa_S) & 0 \\ 0 & 0 & \kappa_S & -(\delta_S+\alpha) \end{bmatrix}.$$

Let $a_1 = \kappa_H + \mu_H,\ a_2 = 0, a_3 = 0, a_4 = \frac{\beta_H\theta_C\Lambda_H}{\delta_C C_0\delta_H}$

In the same manner,

$b_1 = \kappa_H,\ b_2 = \mu_H + \delta_H + \gamma_H,\ c_2 = \frac{\beta_S\theta_M\Lambda_S}{\delta_M M_0\delta_C},\ c_3 = \delta_S + \alpha + \kappa_S,\ d_3 = \kappa_S,\ d_4 = \delta_S + \alpha$

The eigenvalues are solutions of the characteristic equation of the reduced matrix of dimension four which is given by

$$(\kappa_H+\mu_H+\lambda)[(\mu_H+\delta_H+\gamma_H+\lambda)(\delta_S+\alpha+\kappa_S+\lambda)(\delta_S+\alpha+\lambda)] - \frac{\kappa_H\kappa S\beta_H\theta_C\Lambda_H\beta_S\theta_M\Lambda_S}{\delta_C C_0\delta_H\delta_M M_0\delta_S}\Bigg) = 0$$

which is simplified to

$$\begin{aligned} &\lambda^4 + A_3\lambda^3 + A_2\lambda^2 + A_1\lambda + A_0 = 0, \\ &A_3 = a_1 + b_2 + c_3 + d_4, \\ &A_2 = (a_1 + d4)(b_2 + c_3) + a_1 d_4 + b_2 c_3, \\ &A_1 = c_3 d_4(b_2 + a_1) + a_1 b_2(c_3 + d_4), \\ &A_0 = (\kappa_H+\mu_H)(\delta_S+\alpha\kappa_S)(\delta_S+\alpha)(\mu_H+\delta_H+\gamma_H) - \frac{\kappa_H\kappa S\beta_H\theta_C\Lambda_H\beta_S\theta_M\Lambda_S}{\delta_C C_0\delta_H\delta_M M_0\delta_S}. \end{aligned} \tag{6}$$

The Routh–Hurwitz conditions are sufficient and necessary conditions on the coefficients of the polynomial (6). These conditions ensure that all roots of the polynomial given by (6) have negative real parts. For this polynomial, the Routh–Hurwitz conditions are $A_3 > 0, A_2 > 0, A_1 > 0, A_0 > 0$ and

$$H_1 = A_3 > 0,$$

$$H_2 = \begin{vmatrix} A_3 & 1 \\ A_1 & A_2 \end{vmatrix} > 0,$$

$$H_3 = \begin{vmatrix} A_3 & 1 & 0 \\ A_1 & A_2 & A_3 \\ 0 & A_0 & A_1 \end{vmatrix} > 0,$$

$$H_4 = \begin{vmatrix} A_3 & 1 & 0 & 0 \\ A_1 & A_2 & A_3 & 1 \\ 0 & A_0 & A_1 & A_2 \\ 0 & 0 & 0 & A_0 \end{vmatrix} > 0,$$

since all $A_i > 0,\ i = 1, 2, 3.$

Note that from

$$A_0 = (\kappa_H + \mu_H)(\delta_S + \alpha\kappa_S)(\delta_S + \alpha)(\mu_H + \delta_H + \gamma_H) - \frac{\kappa_H\kappa_S\beta_H\theta_C\Lambda_H\beta_S\theta_M\Lambda_S}{\delta_c C_0\delta_H\delta_M M_0\delta_S} > 0$$

we deduce the reproduction number

$$\mathcal{R}_s^2 = \frac{\kappa_H\kappa_S\beta_H\theta_C\Lambda_H\beta_S\theta_M\Lambda_S}{\delta_c C_0\delta_H\delta_M M_0\delta_S(\kappa_H + \mu_H)(\delta_S + \alpha + \kappa_S)(\delta_S + \alpha)(\mu_H + \delta_H + \gamma_H)},$$

which satisfies $\mathcal{R}_s < 1$, in order to have $A_0 > 0$.

Clearly, $H_1 = A_3 > 0$.

$$\begin{aligned} H_2 &= A_3A_2 - A_1 \\ &= (b_2 + c_3)(b_2 + d_4)(c_3 + d_4) + a_1^2(b_2 + c_3 + d_4) + a_1(b_2 + c_3 + d_4)^2 \end{aligned} \tag{7}$$

which is positive.

$$\begin{aligned} H_3 &= A_1(A_3A_2 - A_1) - A_0A_3^2 \\ &= a_1^3(b_2 + c_3)(b_2 + d_4)(c_3 + d_4) + b_2c_3(b_2 + c_3)d_4(b_2 + d_4)(c_3 + d_4) + a_4b_1c_2d_3(b_2 + c_3 + d_4)^2 \\ &\quad + a_1^2(a_4b_1c_2d_3 + b_2^3(c_3 + d_4) + 2b_2^2(c_3 + d_4)^2 + c_3d_4(c_3 + d_4)^2 + b_2(c_3^3 + 4c_3^2d_4 + 4c_3d_4^2 + d_4^3)) \\ &\quad + a_1(b_2^3(c_3 + d_4)^2 + (c_3 + d_4)(2a_4b_1c_2d_3 + c_3^2d_4^2) + b_2^2(c_3^3 + 4c_3^2d_4 + 4c_3d_4^2 + d_4^3) \\ &\quad + 2b_2(a_4b_1c_2d_3 + c_3d_4(c_3 + d_4)^2)) \end{aligned} \tag{8}$$

which is also positive.

It can be easily seen that $H_4 = A_0H_3$.

Therefore, all eigenvalues of the Jacobian matrix have negative real parts when $\mathcal{R}_s < 1$. However, $\mathcal{R}_s > 1$ implies that $A_0 < 0$, and since all coefficients of the polynomial (6) are positive, not all roots of this polynomial can have negative real parts. This means that when $\mathcal{R}_s > 1$, the disease free equilibrium point is unstable. □

3.4. Endemic equilibrium and its stability

The endemic equilibrium point for system (4) in terms of the forces of infection λ_H^* and $\lambda_S^*$is given by

$$\begin{aligned} S_H^* &= \frac{\Lambda_H(\kappa_H + \mu_H)(\mu_H + \delta_H + \gamma_H)}{(\lambda_H^* + \mu_H)(\kappa_H + \mu_H)(\mu_H + \delta_H + \gamma_H) - \gamma_H\kappa_H\lambda_H^*}, \\ E_H^* &= \frac{\lambda_H^*\Lambda_H(\mu_H + \delta_H + \gamma_H)}{\delta_H(\kappa_H + \mu_H)(\lambda_H^* + \mu_H) + \mu_H[(\kappa_H + \mu_H)(\lambda_H^* + \mu_H) + \gamma_H(\kappa_H + \lambda_H^* + \mu_H)]}, \\ I_H^* &= \frac{\kappa_H\lambda_H^*\Lambda_H}{\delta_H(\kappa_H + \mu_H)(\lambda_H^* + \mu_H) + \mu_H[(\kappa_H + \mu_H)(\lambda_H^* + \mu_H) + \gamma_H(\kappa_H + \lambda_H^* + \mu_H)]}, \\ U^* &= \frac{\Lambda_S^*}{\delta_S + \lambda_S^*},\ L^* = \frac{\lambda_S^*\Lambda_S}{(\alpha + \delta_S + \kappa_S)(\delta_S + \lambda_S^*)},\ I_S^* = \frac{\kappa_S\lambda_S^*\Lambda_S}{(\alpha + \delta_S)(\alpha + \delta_S + \kappa_S)(\delta_S + \lambda_S^*)}. \end{aligned} \tag{9}$$

3.4.1. Local stability of the endemic equilibrium

The stability of the endemic equilibrium can be determined by computing the eigenvalues of the Jacobian matrix and then evaluate it at the endemic equilibrium. However this approach is mathematically complicated for the system of Eq. (4). Bifurcation analysis is performed at the disease free equilibrium by using Center Manifold Theory as presented in Castillo-Chavez and Song [16].

Letting $x_1 = S_H,\ x_2 = E_H,\ x_3 = I_H,\ x_4 = U,\ x_5 = L,\ x_6 = I_S$, we write system (4) as

$$\frac{dX_i}{dt} = \mathbf{F}(\mathbf{X}_i)$$

where $X_i = (x_1, x_2, \ldots, x_8)^T$, $\mathbf{F} = (f_1, f_2, \ldots, f_8)^T$ and $(.)^T$ represents the matrices transpose.

The system of Eq. (4) becomes

$$\begin{aligned} \frac{dx_1}{dt} &= f_1 = \Lambda_H - \frac{\beta_H^*\theta_C x_6 x_1}{\delta_S C_0 + \epsilon\theta_C x_6} - \mu_H x_1 + \gamma_H x_3, \\ \frac{dx_2}{dt} &= f_2 = \frac{\beta_H^*\theta_C x_6 x_1}{\delta_S C_0 + \epsilon\theta_C x_6} - (\mu_H + \kappa_H)x_2, \\ \frac{dx_3}{dt} &= f_3 = \kappa_H x_2 - (\mu_H + \delta_H + \gamma_H)x_3, \\ \frac{dx_4}{dt} &= f_4 = \Lambda_S - \frac{\beta_S\theta_M x_3 x_4}{\delta_M M_0 + \epsilon\theta_M x_3} - \delta_S x_4, \end{aligned}$$

$$\frac{dx_5}{dt} = f_5 = \frac{\beta_S\theta_M x_3 x_4}{\delta_M M_0 + \epsilon\theta_M x_3} - (\delta_S + \alpha + \kappa)x_5,$$
$$\frac{dx_6}{dt} = f_6 = \kappa x_5 - (\delta_S + \alpha)x_6, \tag{10}$$

where $\beta_H^* = \beta_H$ from (5). Suppose that β_H^* is a bifurcation parameter, the system (10) is linearised at disease free equilibrium point $\mathcal{E}_0$ when $\beta_H = \beta_H^*$ with $\mathcal{R}_s = 1$. Now solving for $\mathcal{R}_s = 1$ in (5) gives

$$\beta_H^* = \frac{\delta_C C_0 \delta_H M_0 \delta_S(\kappa_H + \mu_H)(\delta_S + \alpha + \kappa_S)(\delta_S + \alpha)(\mu_H + \delta_H + \gamma_H)}{\kappa_H\kappa_S\theta_C\theta_M\beta_S\Lambda_S\Lambda_H}.$$

Then zero is a simple eigenvalue of the following Jacobian matrix with the application of the bifurcation parameters.

$$\begin{bmatrix} -\mu_H & 0 & \gamma_H & 0 & 0 & \frac{-\beta_H^*\theta_C\Lambda_H}{\delta_C C_0\delta_H} \\ 0 & -(\kappa_H+\mu_H) & 0 & 0 & 0 & \frac{\beta_H^*\theta_C\Lambda_H}{\delta_C C_0\delta_H} \\ 0 & \kappa_H & -(\mu_H+\delta_H+\gamma_H) & 0 & 0 & 0 \\ 0 & 0 & \frac{-\beta_S\theta_M\Lambda_S}{\delta_M M_0\delta_S} & -\delta_S & 0 & 0 \\ 0 & 0 & \frac{-\beta_S\theta_M\Lambda_S}{\delta_M M_0\delta_S} & 0 & -(\delta_S+\alpha+\kappa_S) & 0 \\ 0 & 0 & 0 & 0 & \kappa_S & -(\delta_S+\alpha) \end{bmatrix}.$$

A right eigenvector associated with the eigenvalue zero is $\omega = (\omega_1, \omega_2, \ldots, \omega_6)$, where

$$\omega_1 = \frac{\gamma_H\omega_3 + \beta_H^* Q_1\omega_6}{\mu_H},\ \omega_2 = \frac{\beta_H^* Q_1\omega_6}{\kappa_H + \mu_H},\ \omega_3 = \frac{\kappa_H\omega_2}{\mu_H + \delta_H + \gamma_H},$$
$$\omega_4 = \frac{-\beta_S Q_2\omega_3}{\delta_S},\ \omega_5 = \frac{\beta_S Q_2\omega_3}{\delta_S + \alpha + \kappa_S},\ \omega_6 = \frac{\kappa_S\omega_5}{\delta_S + \alpha}. \tag{11}$$

The left eigenvector satisfying $v.\omega = 1$ is $v = (v_1, v_2, \ldots, v_6)$, where $v_1 = 0,\ v_2 = v_2 > 0,\ v_3 = \frac{(\kappa_H+\mu_H)v_2}{\kappa_H}$,
$v_4 = 0,\ v_5 = \frac{\mu_H+\delta_H+\gamma_H}{\beta_S Q_2}v_3,\ v_6 = \frac{\beta_H^* Q_1}{\delta_S+\alpha}v_2$.

Theorem 4.1 in Castillo-Chavez and Song [16] is used to explore local stability of the endemic equilibrium near $R_s = 1$.

***Computation of* $\mathbf{a_{cs}}$ *and* $\mathbf{b_{cs}}$**

For the system (10), the associated non-zero second order partial derivatives at disease free equilibrium are given by

$$a_{cs} = \sum_{k,i,j=2}^{3} v_k\omega_i\omega_j \frac{\partial^2 f_k}{\partial x_i \partial x_j}(0,0) + \sum_{k,i,j=5}^{6} v_k\omega_i\omega_j \frac{\partial^2 f_k}{\partial x_i \partial x_j}(0,0),$$

$$b_{cs} = \sum_{k,i=2}^{3} v_k\omega_i \frac{\partial^2 f_k}{\partial x_i \partial \phi}(0,0) + \sum_{k,i=5}^{6} v_k\omega_i \frac{\partial^2 f_k}{\partial x_i \partial \phi}(0,0).$$

Since $v_k = 0$, for $k = 1, 4$, we should consider v_k for $k = 2, 3, 5, 6$.

That is, the following functions will be used to find a_{cs} and b_{cs} from the system (10).

$$f_2 = \frac{\beta_H^*\theta_C x_6 x_1}{\delta_S C_0 + \epsilon\theta_C x_6} - (\kappa_H + \mu_H)x_2,$$
$$N_H = x_1 + x_2 + x_3$$
$$f_2 = \frac{\beta_H^*\theta_C x_6(N_H - x_2 - x_3)}{\delta_S C_0 + \epsilon\theta_C x_6} - (\kappa_H + \mu_H)x_2. \tag{12}$$

Hence

$$\frac{\partial^2 f_2}{\partial x_2 \partial x_6} = -\frac{\beta_H^*\theta_C}{\delta_S C_0} = \frac{\partial^2 f_2}{\partial x_3 \partial x_6},$$

$$f_5 = \frac{\beta_S\theta_M x_3 x_4}{\delta_M M_0 + \epsilon\theta_M x_3} - (\delta_S + \alpha + \kappa_S)x_5$$
$$N_S = x_4 + x_5 + x_6,$$
$$f_5 = \frac{\beta_S\theta_M x_3(N_S - x_5 - x_6)}{\delta_M M_0 + \epsilon\theta_M x_3} - (\delta_S + \alpha + \kappa_S)x_5, \tag{13}$$

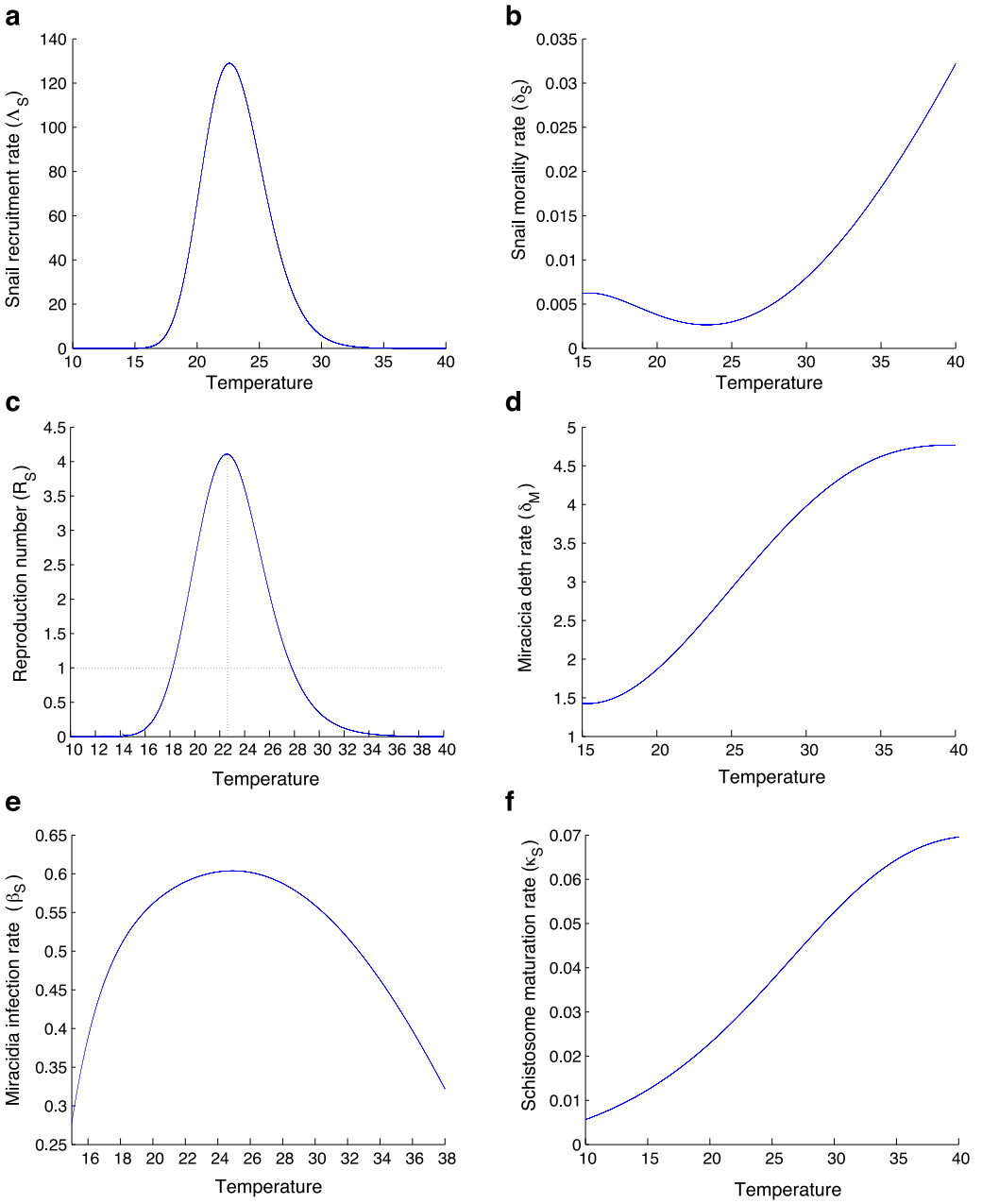

Fig. 2. Simulation of (a) Snail egg laying rate, (b) Snail mortality rate, (c) R_s, (d) Miracidia death rate, (e) Miracidia infection rate and (f) within snail schistosome maturation rate using parameter functions in Table 1.

hence

$$\frac{\partial^2 f_5}{\partial x_5 \partial x_3} = -\frac{\beta_S \theta_M}{\delta_M M_0} = \frac{\partial^2 f_5}{\partial x_6 \partial x_3}.$$

Therefore on simplifying we get

$$a_{cs} = -\frac{(\beta_H^*)^2 \theta_C Q_1 (\mu_H + \delta_H + \gamma_H + \kappa_H)}{\delta_S C_0 (\kappa_H + \mu_H)(\mu_H + \delta_H + \gamma_H)} v_2 \omega_6^2 - \frac{\beta_S^2 \theta_M Q_2 (\delta_S + \alpha + \kappa_S)}{\delta_M M_0 (\delta_S + \alpha)(\delta_S + \alpha + \kappa_S)} v_6 \omega_3^2 < 0.$$

From Eq. (12) we get

$$\frac{\partial^2 f_2}{\partial x_6 \partial \beta_H^*} = \frac{\theta_C \Lambda_H}{\mu_H \delta_S C_0}.$$

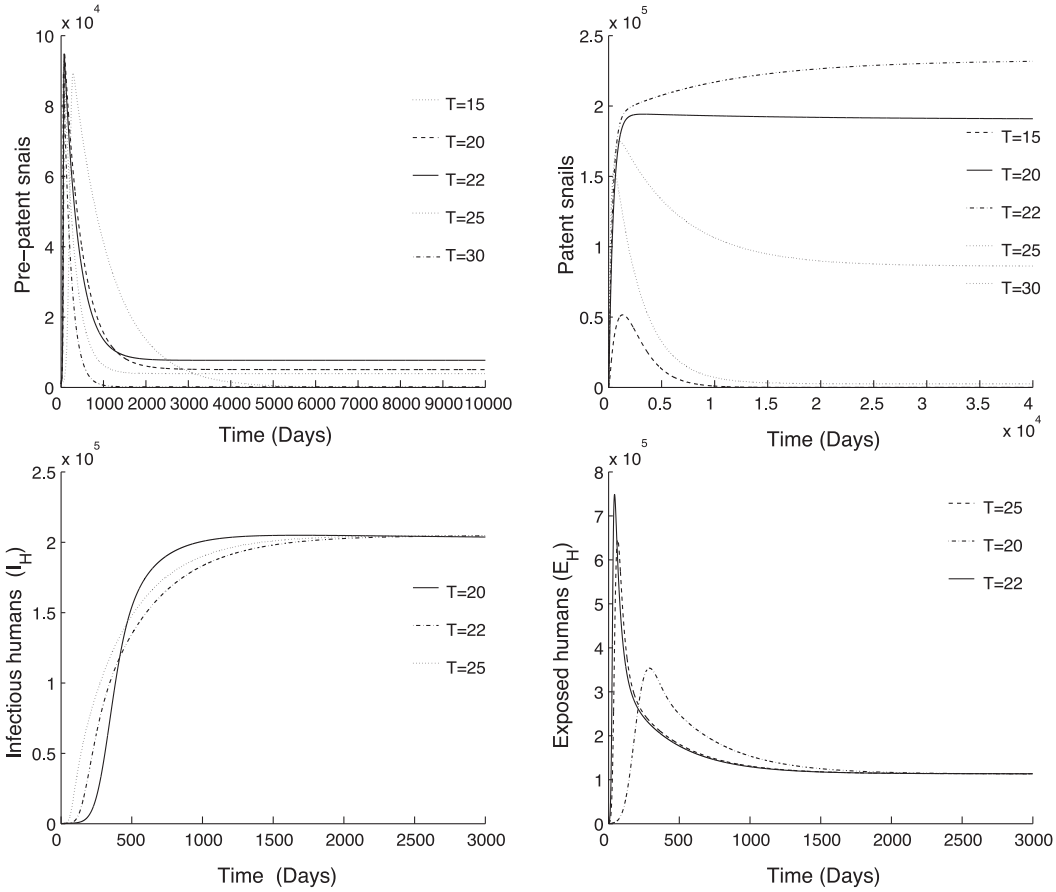

Fig. 3. Simulation of infected snails and human populations with varying temperature, using model system (2).

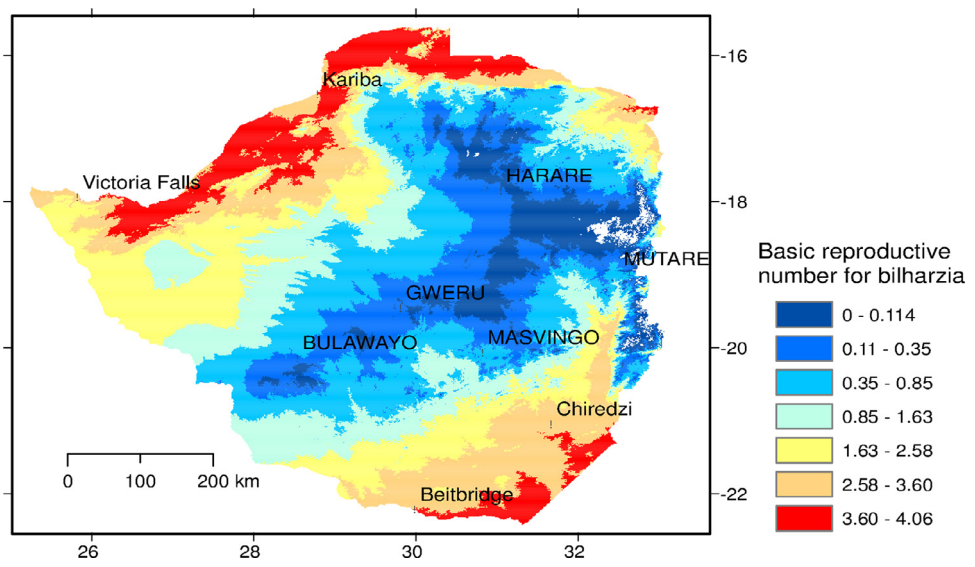

Fig. 4. Variation of reproduction number R_s as a function of temperature in Zimbabwe.

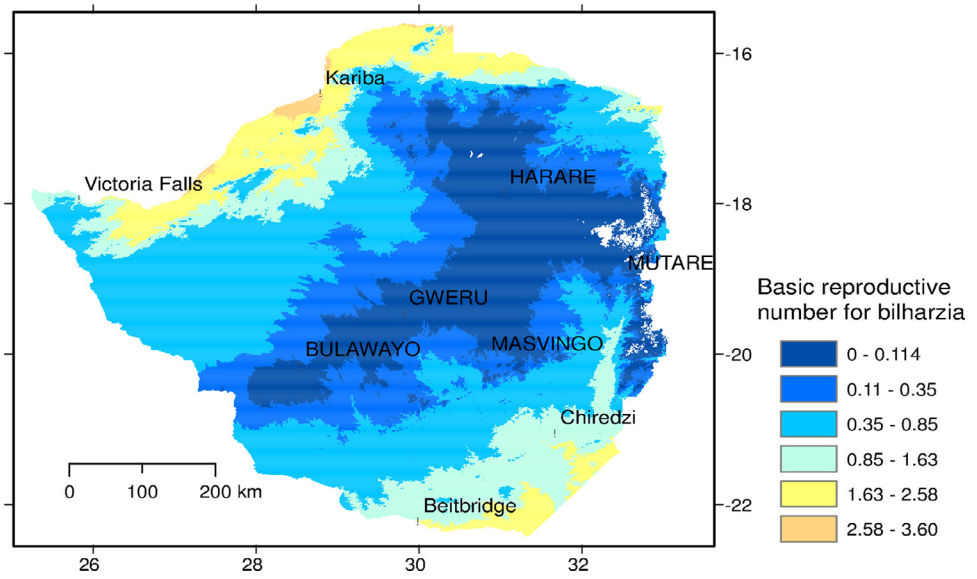

Fig. 5. Variation of reproduction number R_s as a function of temperature and rainfall in Zimbabwe.

Therefore

$$b_{cs} = \frac{\theta_C \Lambda_H}{\mu_H \delta_S C_0} \nu_2 \omega_6 > 0.$$

Thus $a_{cs} < 0$ and $b_{cs} > 0$ and the following theorem follows:

Theorem 2. *The unique endemic equilibrium $\mathcal{E}^*$ guaranteed by Theorem 4.1 (Castillo-Chavez and Song [17]) is locally asymptotically stable for $\mathcal{R}_s > 1$, but close to 1.*

4. Numerical simulations

We explore the effects of temperature and rainfall using graphical representations.

In Fig. 2, the effects of temperature on snail recruitment rate, snail mortality rate, basic reproduction number, miracidia death rate, miracidia infection rate and within snail schistosome maturation rate are illustrated. The snail recruitment rate is 0 at 15 °C and increases to a maximum at around 23 °C before declining to zero again at around 34 °C. This is in agreement with Dagal et al. [8] because no snail eggs hatch at temperatures lower than 15 °C and at temperatures greater or equal to 35 °C. The snail recruitment rate is maximum at 24 °C as the optimal temperatures for reproduction lie between 22 °C and 26 °C, in agreement with WHO [1]. Snail mortality is high at low temperatures but decreases to a minimum between 20 °C and 25 °C before increasing again at higher temperatures. The reproduction number is zero at 10 °C and increases to become greater than unity around 18 °C. It increases to a maximum at about 22.5 °C before declining to zero at about 35 °C. The reproduction number is greater than unity between 18 °C and 28 °C making this temperature range the ideal temperature range for endemic schistosomiasis.

In Fig. 3, the relationship between pre-patent snails, patent snails, exposed humans and infectious humans is illustrated. Results show that in the long term, the effects of temperature within the range 20–25 °C on human infectivity is more or less constant.

Fig. 4 shows different reproduction numbers across Zimbabwe. Cooler and warmer colours represent low and high reproduction numbers, respectively. Thus based on temperature alone highest reproduction numbers are in the lower veld and the Zambezi valley catchment area. Higher reproduction numbers signify higher incidences of schistosomiasis. Based on these results which are temperature dependant, it is shown that most major towns have very low incidence of schistosomiasis if we are to base the results on temperature only.

In Fig. 5, the combined effects of temperature and rainfall patterns in Zimbabwe from 1950 to 2000 were used to map the reproduction number risk map for schistosomiasis transmission. As the intensity of the colour increases, the reproduction number also increases. Therefore, high reproductive numbers are found in the lower veld of Zimbabwe and along the Zambezi valley catchment area. This correlates with high incidence of schistosomiasis. This result is in total agreement with Midzi et al. [17] who obtained similar results for the cross-sectional survey of 280 primary schools country wide. The combined effect of rainfall and temperature seem to lower the reproduction number as the reproduction number is a decreasing function of rainfall.

5. Discussion

In this paper, a mathematical model to explore the impact of temperature and water bodies taken in the context of rainfall on schistosomiasis transmission is presented as a system of differential equations and analysed. In agreement with Dagal et al. [8], the model analysis suggests that the temperature range of 18–28 °C is found to be ideal for schistosomiasis transmission. The reproduction number increases as temperature increases to attain a maximum around 23 °C, beyond which the reproduction number starts declining. This result suggests the optimal temperature for schistosomiasis transmission is around 23 °C. The analysed results are also supported by numerical simulations which show an increased infection among snails at 22 °C as compared to at 20 °C and 25 °C. At 30 °C the infection dies out. Amongst humans however, the infection is endemic from 20 to 25 °C and the differences in transmission in relation to temperatures are minimal. Geographical information systems (GIS) was used to map the reproduction number on the Zimbabwe map using temperature and rainfall data from 1950 to 2000. It was noted that high reproduction numbers are found in the Zambezi valley catchment area and the lower veld of the country. High reproduction numbers suggest high incidences of schistosomiasis. The results of this manuscript can be used to identify areas which need special attention with regard to schistosomiasis control. Chiredzi, a known irrigated sugarcane producing area and Mushandike areas in the Lowveld of Zimbabwe are among those requiring special attention in the fight against schistosomiasis. This manuscript can be extended to incorporate other aspects like the terrain of the country under study to capture the real dynamics of what happens on the ground.

References

[1] World Health Organisation, 2015. http://www.who.int/mediacentre/factsheets/fs115/en/ [accessed May 2015].
[2] Ukoroije BR, Abowei JFN. Some occupational diseases in culture fisheries management and practices part two: schistosomiasis and filariasis. Int J Fishes Aquat Sci 2012;1(1):64–71.
[3] Chitsulo L, Angels D, Montressor A, Savioli L. The global status of schistosomiasis and its control. Acta Tropica 2000;77:41–51.
[4] Sturrock RF. The intermediate hosts and host-parasite relationships. In: Jordan P, Webbe G, Sturrock RF, editors. Human Schistosomiasis. Wallingford: CAB International; 1993. p. 33–85.
[5] De jesus AR, Gonzalez Miranda D, Gonzalez Miranda R, Arau Jo I, Andrea Magalha ES, Bacellar M, et al. Morbidity associated with schistosoma mansoni infection determined by ultrasound in an endemic area of Brazil. Am Soc Trop Med Hyg 2000;63:1–4.
[6] WHO Expert Committee. Prevention and control of schistosomiasis and soil-transmitted helminthiasis. World Health Organ Technical Report Series 2002;912:1–57.
[7] Brooker S. Spatial epidemiology of human schistosomiasis in Africa: risk models, transmission dynamics and control. Trans R Soc Trop Med Hyg 2007;101:1–8.
[8] Dagal MA, Upatham ES, Kruatrache M, Viyanant V. Effects of some physico-chemical factors on the hatching of egg masses and on the survival of juvenile and adult snails of bulinus (physopsis) abyssinicus. ScienceAsia 1986;12:23–30.
[9] Cohen JE. Mathematical models of schistosomiasis. Annu Rev Ecol Syst 1977;8:209–33.
[10] Spira AM. Assessment of travelers who return home ill. The Lancet 2003;361:1459–69.
[11] Chiyaka E, Garira W. Mathematical analysis of the transmission dynamics of schistosomiasis in the human-snail hosts. J Biol Syst 2009;17:397–423.
[12] Feng Z, Li CC, Milner FA. Schistosomiasis models with density dependence and age of infection in snail dynamics. Math Biosci 2002;177:271–86.
[13] Liang S, Spear RC, Seto E, Hubbard A, Qui D. A multi-group model of schistosoma japonicum transmission dynamics and control: model calibration and control prediction. Trop Med Int Health 2005;3:263–78.
[14] Mangal TD, Paterson S, Fenton A. Predicting the impact of long-term temperature changes on the epidemiology and control of schistosomiasis: a mechanistic model. PLoS ONE 2008;3(1):e1438. doi:10.1371/journal.pone.0001438.s001.
[15] Diekmann O, Heestterbeek JAP, Metz JAJ. On the computation of the basic reproduction ratio r_0 in models for infectious diseases in heterogenous populations. J Math Biol 1990;28:365–82.
[16] Castillo-Chavez C, Song B. Dynamical models of tuberculosis and their applications. Math Biosci Eng 2004;1:361–404.
[17] Midzi N, Mduluza T, Chimbari MJ, Tshuma C, Charimari L, Mhlanga G, et al. Distribution of schistosomiasis and soil transmitted helminthiasis in Zimbabwe: towards a national plan of action for control and elimination. PLoS Negl Trop Dis 2014;8(8):e3014. doi:10.1371/journal.pntd.0003014.